

Segregation of RNA and Separate Packaging of DNA and RNA in Apoptotic Bodies during Apoptosis

H. Dorota Halicka,* Elzbieta Bedner,*† and Zbigniew Darzynkiewicz*¹

*Brander Cancer Research Institute, New York Medical College, Hawthorne, New York 10532; and †Department of Pathology, Pomeranian School of Medicine, Szczecin, Poland

Apoptosis is characterized by a complex and remarkably ordered choreography of events consisting of the preparatory and execution steps that all culminate in disposal of the cell remnants. The disposal occurs in a manner that is the least destructive to the tissue: the remains of nuclear chromatin and cytoplasm are packaged in apoptotic bodies which are then phagocytized by neighboring live cells without invoking inflammatory or autoimmune response. In the present study we describe that in the course of apoptosis cellular RNA becomes sequestered and packaged into granules and then into apoptotic bodies, separately from DNA. This separation, which appears to be initiated by the nucleolar segregation, was observed in HL-60 cells that were undergoing spontaneous apoptosis in cultures or were treated with the DNA-damaging drug, DNA topoisomerase I inhibitor camptothecin (CPT), or with the cell death ligand, tumor necrosis factor- α . RNA separation was also observed in apoptotic MCF-7 cells following treatment with CPT. RNA and DNA in apoptotic cells were identified histochemically, by their differential stainability with pyronin Y and Hoechst 33342 fluorochromes, respectively, and immunocytochemically, by labeling the RNA with BrU for various periods of time and detection of the incorporated precursor with fluoresceinated anti-BrU mAb; DNA was counterstained with 7-aminoactinomycin D. Over 90% of apoptotic bodies that contained RNA had no detectable DNA and vice versa, the apoptotic bodies containing DNA had no detectable RNA. Packaging RNA and DNA into separate apoptotic bodies suggests that the phagosomes of the cells that ingest these particles are specialized: some of them are responsible for DNA degradation, others for degradation of RNA. Such specialization may facilitate heterophagic degradation of nucleic acids during apoptosis. © 2000 Academic Press

Key Words: camptothecin; TNF- α ; laser scanning cytometry; pyronin Y; incorporation of BrU; apoptotic bodies; nucleolus; caspase activation; phagocytosis.

¹ To whom reprint requests should be addressed. Fax: (914) 347-2804. E-mail: darzynk@nymc.edu.

INTRODUCTION

One of the most characteristic features of apoptosis is orderly disposal of cell remnants. The disposal takes place through cell fragmentation into apoptotic bodies; the latter are engulfed by the neighboring cells that do not necessarily have to be professional phagocytes (for reviews, [1–4]). Phagocytosis is enabled by a change in the plasma membrane of the dying cell that leads to exposure of phosphatidylserine on the outer leaflet of the membrane [5]. This phospholipid provides a signal that attracts adjacent live cells and provokes them to engulf the dead cell remnants. With no leakage of the cytosol constituents into the intercellular space there is no inflammatory response to cell death and no scar formation [1–4].

An important step in cell disposal is degradation of nucleic acids [1–4, 6]. The mechanism of cell-autonomous DNA degradation during apoptosis has been extensively studied. For a long time conflicting reports appeared regarding involvement of different endonucleases in this process (e.g., [7, 8]). Recent findings, however, provided convincing evidence that the caspase-activated DNase (CAD) is one of the main nucleases that degrades chromosomal DNA during apoptosis (for review, [9]). This endonuclease is well conserved during evolution (75.9% identity between human and mouse) but has no homology with DNase I or DNase II [9]. In live cells CAD remains in a complex with its chaperone protein and the inhibitor ICAD [9–11]. Activation of caspase-3 leads to cleavage of the ICAD complex thereby releasing active CAD, which initiates fragmentation of DNA. The DNA is initially cleaved to large fragments of 50 to 300 kb in size. Subsequently, DNA undergoes fragmentation to oligo- and mononucleosomal (180 bp) sections [6]. Upon ingestion of the apoptotic bodies further DNA degradation takes place in lysosomes of the phagocyte [12–14]. Several nucleases, identified in the nematode *Caenorhabditis elegans* as products of the NUC-1, CED-2, CED-5, CED-6, and CED-10 genes, continue heterophagic DNA degradation up to completion [12, 13].

Compared to DNA degradation the disposal of RNA

during apoptosis has been studied less extensively. The interferon-induced 2',5'-oligoadenylate-activated ribonuclease L (RNase L, 2',5'-A-dependent RNase L) appears to be the enzyme that specifically degrades rRNA during apoptosis in different cell systems [15, 16]. While 18S rRNA is not cleaved by this nuclease, 28S rRNA is cleaved at several specific sites [17]. As would be expected, the degradation of a 28S rRNA occurs simultaneous with a cessation of protein synthesis [18]. However, whereas the caspase-3 inhibitor Z-DEVD-FMK was seen to prevent rRNA degradation upon induction of apoptosis by anti-FAS antibody in Jurkat cells, it had no effect on rRNA degradation in U-937 cells triggered to apoptosis by tumor necrosis factor α (TNF- α) [18]. Apparently, different pathways may be used to activate RNase L during apoptosis in different cell systems.

There is evidence in the literature that ribonucleoprotein (RNP) complexes are extruded from the cells undergoing apoptosis as separate structures. Namely, using histochemical procedure to detect RNA (terbium citrate) Biggiogera *et al.* [19] observed that during spontaneous apoptosis of rat thymocytes RNA was initially removed from the nucleus, clustered within the cytoplasm in separate areas, and then released at the cell surface in the form of minute membrane-bounded blebs. The proteins of RNP, detected immunocytochemically, showed similar localization [20].

In the present study, using methodology and cell systems different from those of Biggiogera *et al.* [19, 20], we provide further evidence of RNA separation during apoptosis. We also identify two types of apoptotic bodies: those that contain RNA but have no DNA and those that contain only DNA. Two means of RNA vs DNA identification were used. In the first method cellular RNA was labeled with BrU by growing the cells in the presence of BrU for different periods of time. The incorporated (sensitive to RNase) BrU was then immunocytochemically detected using anti-BrU mAb [21–23] while DNA was counterstained with 7-aminoactinomycin D (7-AAD) and fluorescence intensity was measured by laser scanning cytometry (LSC; Refs. [26, 27]). In the second method RNA and DNA were differentially stained with pyronin Y and Hoechst 33342, respectively [24, 25]. These fluorochromes were visualized within the cell by fluorescence microscopy. The data show that RNA and DNA were specifically segregated and packaged into different chromatin granules which ultimately formed separate apoptotic bodies. We hypothesize that separation of DNA and RNA in distinct apoptotic bodies may facilitate their efficient heterophagic degradation in phagosomes. The latter may be specialized in terms of providing optimal ionic and enzymatic environment for complete degradation of either RNA or DNA.

MATERIALS AND METHODS

Cells. Human promyelocytic leukemic HL-60 cells obtained from the American Type Culture Collection (Rockville, MD) were maintained in RPMI 1640 supplemented with 10% fetal calf serum, 100 units/ml penicillin, 100 mg/ml streptomycin, and 2 mM L-glutamine (all from Gibco BRL Life Technologies, Inc., Grand Island, NY). At the onset of experiments there were fewer than 5×10^5 cells per 1 ml in cultures and the cells were at an exponential and asynchronous phase of their growth. The cultures were maintained at 37.5°C in an atmosphere of 5% CO₂ in air. The human breast carcinoma cell line MCF-7 was also obtained from the ATCC and the cells were grown in two-chamber microscope slide tissue culture vessels (Lab-Tek; Nalge Nunc, Naperville, IL) as described elsewhere [28]. In order to label cellular RNA the cells were incubated in the presence of BrU (Sigma Chemical Co., St. Louis, MO) included in the culture medium for various periods of time from 20 min to 14 h as specified in the figure legends. At shorter incubation times with BrU (20 min–2 h) the precursor was added to obtain 1 mM as its final concentration in the culture. With longer incubation times (>2 h) BrU was at 0.2 mM concentration. Incubations with BrU and further handling of the BrU-labeled cells up to the point when they were fixed were carried out in dimmed light and the tissue culture flasks and centrifuge tubes containing cell suspensions were wrapped in aluminum foil to minimize cells' exposure to light.

Induction of apoptosis. Exponentially growing HL-60 cells in 25-ml flasks were treated with either 0.15 μ M DNA topoisomerase I inhibitor camptothecin (CPT) (Sigma Chemical Co.) or a combination of 0.3 nM TNF- α and 5 μ M cycloheximide (CHX; both from Sigma) for up to 6 h. MCF-7 cells were treated with 0.15 μ M CPT for up to 48 h. HL-60 cells were harvested at different times after drug administration as specified in the figure legends. For further analysis by LSC HL-60 cells were attached to microscope slides using the cytocentrifuge (Shandon, Inc., Pittsburgh, PA; 1000 rpm, 6 min, room temperature) and the slides were fixed in ice-cold 1% solution of methanol-free formaldehyde (Polysciences, Inc., Warrington, PA) in PBS for 15 min and postfixed in cold 70% ethanol for at least 2 h or stored at –20°C. Other details of cell preparation for analysis by microscopy and by LSC are presented elsewhere [28, 29]. For analysis of RNA or DNA presence in apoptotic bodies under fluorescence microscope the cells were cytocentrifuged at 1500 rpm for 10 min and fixed as above.

Immunocytochemical detection of BrU-labeled RNA. After fixation in formaldehyde followed by 70% ethanol the slides were rinsed in PBS and the cells were incubated with the mouse anti-BrU mAb (clone PRB1-U, IgG1 κ type; Phoenix Flow Systems, Inc., San Diego, CA). This antibody is advertised by the vendor as an anti-BrU mAb but it does cross-react with BrU and can be used to detect RNA that has U substituted by BrU [22]. The anti-BrU mAb was used at 1 μ g/100 μ l concentration in a solution of 1% (w/v) bovine serum albumin (BSA) in PBS and the cells were incubated with it overnight at 4°C. The slides were then rinsed with 1% BSA in PBS and incubated with the FITC-labeled goat anti-mouse antibody (DAKO, Inc., Carpinteria, CA) at 1:30 titer for 30 min at room temperature in the dark. Some slides prior to labeling with anti-BrU mAb were incubated with 200 μ g/ml DNase-free RNase A (Sigma) dissolved in PBS.

Histochemical detection of DNA and RNA. Following the immunocytochemical detection of the incorporated BrU the cellular DNA was counterstained with 5 μ g/ml 7-AAD (Molecular Probes, Inc., Eugene, OR) dissolved in PBS, for 10 min at room temperature. In other cell preparations cellular DNA and RNA were differentially stained with 2 μ g/ml Hoechst 33342 and 20 μ g/ml pyronin Y (both from Molecular Probes), respectively, as described before [25].

Fluorescence measurement. The slides containing cells whose RNA was detected immunocytochemically and whose DNA was stained with 7-AAD were mounted with Vectashield (Vector Labora-

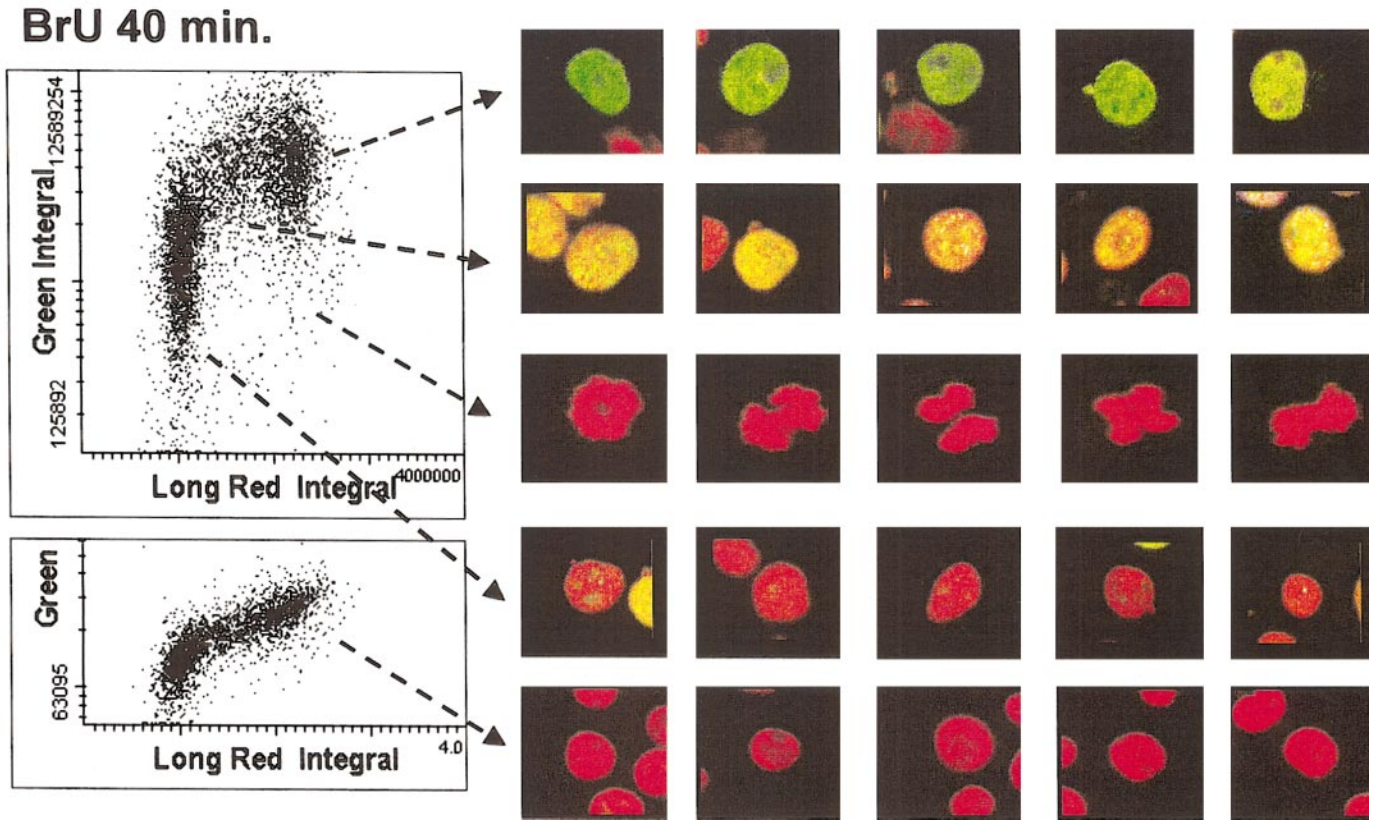


FIG. 1. Differential labeling of cellular DNA and RNA and measurement by laser scanning cytometer (LSC). Following 40 min incubation with 1 mM BrU HL-60 cells were fixed and permeabilized and the incorporated BrU was detected immunocytochemically using anti-BrU mAb followed by secondary fluoresceinated Ab (green fluorescence) as described under Materials and Methods. Cellular DNA was counterstained with the fluorescing red 7-AAD. Intensity of red and green fluorescence was measured by LSC. As is evident from the top scattergram the cells most intensely incorporating BrU were in late S and G_2 ; upon relocation by LSC [26, 27] they had largest nuclear size and showed distinct green fluorescence (top row of cell gallery). Mid-S-phase cells incorporated less BrU and had yellow fluorescence (second row). Mitotic cells (third row) showed no BrU incorporation while early G_1 cells (fourth row) had minimal, punctate, BrU immunofluorescence. The cells that were pretreated with RNase A (bottom scatterplot and bottom row) showed no reactivity at all with anti-BrU mAb.

atories, Burlingame, CA) anti-fade mounting medium under the coverslips and the fluorescence of individual cells was measured by LSC (CompuCyte, Cambridge, MA). Fluorescence of FITC and 7-AAD was excited by 488-nm argon ion laser and emission of those fluorochromes was measured in the green and far red wavelengths, respectively, using standard optical settings of the instrument. At least 5000 cells were analyzed per sample. Other details of cell analysis by LSC were presented before [28, 29]. To quantify the percentage of apoptotic bodies containing segregated RNA and DNA the slides were analyzed under fluorescence microscope (Nikon Microphot FXA, Obj. 40 \times) using mixed illumination, interference (Nomarski) contrast, and either blue or green excitation light, as described in legends to Fig. 5 and Table 1. At least 200 apoptotic bodies per slide from triplicate cultures were analyzed to obtain the means \pm SE shown in Table 1.

RESULTS

The initial experiments were designed to test efficiency and specificity of immunocytochemical detection of RNA using the RNA precursor BrU and mAb that

reacts with the incorporated BrU. This methodology is relatively new and only few reports on its use have appeared to date [21–23, 30]. It should be stressed that not all commercially available anti-BrdU antibodies cross-react with BrU and therefore not all can be used in studies of RNA. Figure 1 illustrates the pattern of cells' labeling following a 40-min pulse with BrU. The cellular DNA was counterstained with 7-AAD and intensity of cell green (FITC) and red (7-AAD) fluorescence was measured by LSC. The differential staining of DNA and RNA allowed us to correlate incorporation of BrU with the cell cycle position. It is evident the cells were very heterogeneous in terms of BrU incorporation. Maximally labeled were the S- and G_2 /M-phase cells, minimally some cells in G_1 and mitotic cells. This pattern of the cell transcriptional activity in relation to its cell cycle position correlates inversely with the degree of nuclear chromatin condensation, which was shown to be minimal in late S and maximal in mitotic

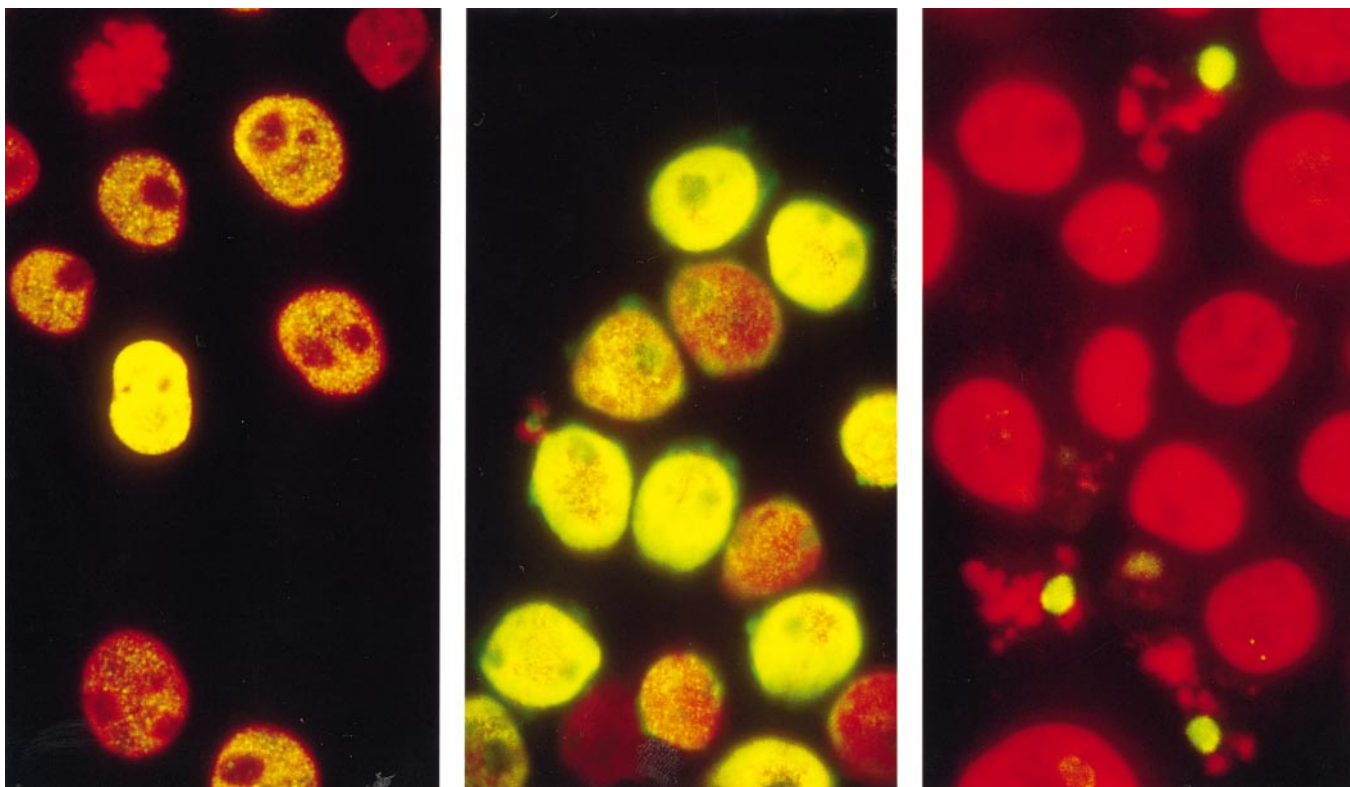


FIG. 2. Incorporation of BrU after a 30-min pulse (left), 3-h pulse (middle), and 30-min pulse of BrU followed by 3 h cell growth of HL-60 cells in BrU-free medium (right). A short pulse of BrU labeled predominantly RNA in nucleoplasm with little incorporation of the precursor into nucleoli (left). Nucleolar RNA was labeled more intensely after a longer pulse of BrU (middle). Nearly all BrU was lost from live cells when the short pulse was followed by a 3-h chase in the BrU-free medium (right). Note, however, that the incorporated BrU remained in distinct chromatin granules of the three cells that had fragmented nucleus, typical of apoptosis. These cells were undergoing spontaneous apoptosis in the culture.

and postmitotic cells [31]. Essentially all green (FITC) fluorescence was sensitive to RNase (Fig. 1, bottom).

Figure 2 shows localization of BrU-labeled RNA in HL-60 cells that were incubated with BrU for 30 min (left), 3 h (middle), or 30 min followed by 3 h growth in BrU-free medium (right). Preferential nucleoplasmic and nucleolar incorporation of BrU was evident in live cells that were treated for 30 min and 3 h with the RNA precursor, respectively. Approximately 5% of HL-60 cells undergo spontaneous apoptosis in cultures. Three apoptotic cells, each having fragmented nucleus with condensed chromatin, a typical sign of apoptosis, are seen in the photomicrograph of the cells from the culture that was pulse-exposed to BrU for 30 min and harvested 3 h later (in Fig. 2, right). It is quite evident that almost all BrU was lost from the live cells. The incorporated BrU, however, remained in the form of a single granule in each of these apoptotic cells. Preincubation of these samples with RNase abolished their reaction with the anti-BrU mAb (not shown). Similar distribution of BrU (one or two granules per cell) was seen in the cells that were undergoing spontaneous

apoptosis in cultures labeled with BrU for various periods of time, from 20 min to 14 h (not shown).

Figure 3 illustrates separation of RNA from DNA during apoptosis when RNA and DNA were differentially stained with pyronin Y and Hoechst 33342 [24, 25]. Apoptosis of MCF-7 cells was induced by their treatment with CPT. Only the RNA-associated red fluorescence of pyronin Y was excited upon illumination of the specimen with green light (right) while only the DNA-associated blue fluorescence of Hoechst 33342 was excited with UV light (left). It was quite apparent that several granular structures outside the cells, which most likely represent apoptotic bodies, showed red fluorescence of pyronin Y only, which did not colocalize with the blue fluorescence of Hoechst 33342.

In the next series of experiments we pre-labeled cellular RNA with BrU by incubating the cells for 3–12 h with the precursor and then treated them with the inducers of apoptosis, either with CPT or with TNF- α + CHX (Fig. 4). A distinct separation of RNA from DNA and packaging of these nucleic acids into separate granules, which in turn were packaged into sepa-

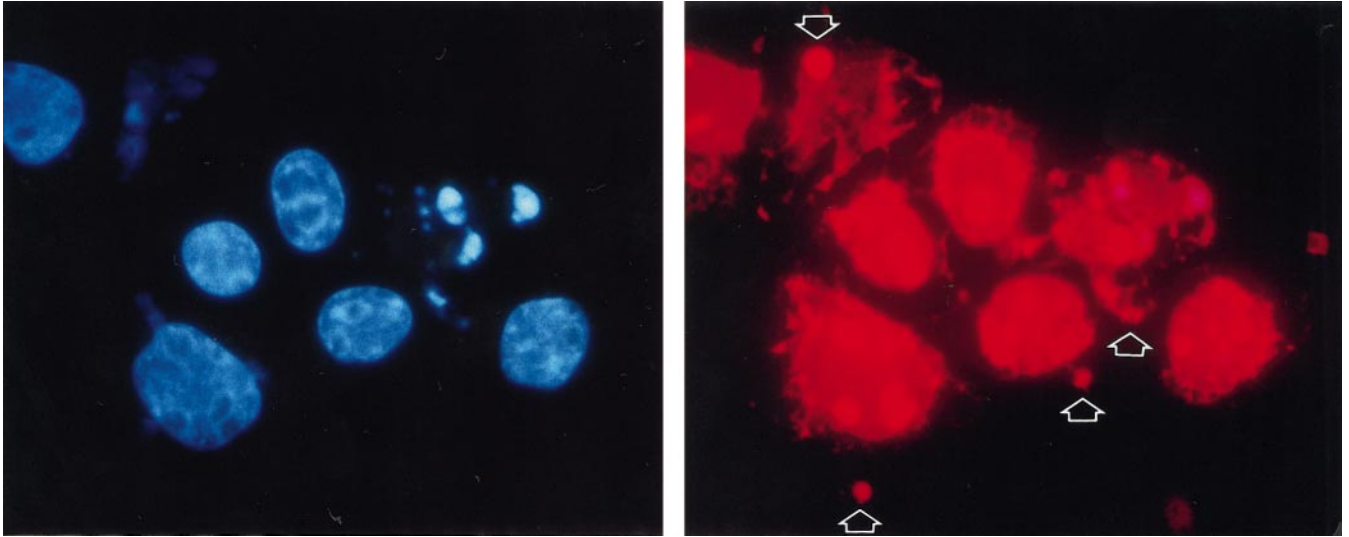


FIG. 3. Separate packaging of RNA and DNA during apoptosis revealed by differential staining of DNA with Hoechst 33342 vs RNA with pyronin Y. Exponentially growing MCF-7 cells were treated with 0.15 μ M CPT for 24 h as described [28]. The cells were then fixed and stained with Hoechst 33342 and pyronin Y, and the same field of view was observed sequentially under fluorescence microscope using either UV (left) or green light (right) illumination. Note that several granular structures resembling nuclear fragments or apoptotic bodies (arrows) stain with pyronin Y (red) but show no Hoechst 33342 (blue) fluorescence.

rate apoptotic bodies, were observed in all cells undergoing apoptosis in these cultures. As is evident in these photomicrographs (Fig. 4) the sequestration of RNA proceeded through the disappearance of RNA from nucleoplasm and its apparent accumulation in one or two sites, often associated with the nucleolus. In the cells that were more advanced in apoptosis and showed nuclear fragmentation the clustered RNA become separated from the nucleoplasm and formed a distinct body(ies). The sequestration of RNA detected by anti-

BrU mAb was observed regardless of the duration of BrU pulse, from 3 to 12 h prior to the addition of the apoptosis-inducing agents.

Other evidence of RNA sequestration and separate packaging into apoptotic bodies is provided in Fig. 5. RNA in HL-60 cells was pre-labeled with BrU and apoptosis was induced by $\text{TNF-}\alpha$ + CHX. Cellular DNA and RNA were detected with 7-AAD and anti-BrU mAb, respectively; the latter was labeled with the FITC-tagged secondary Ab. When the cells were exam-

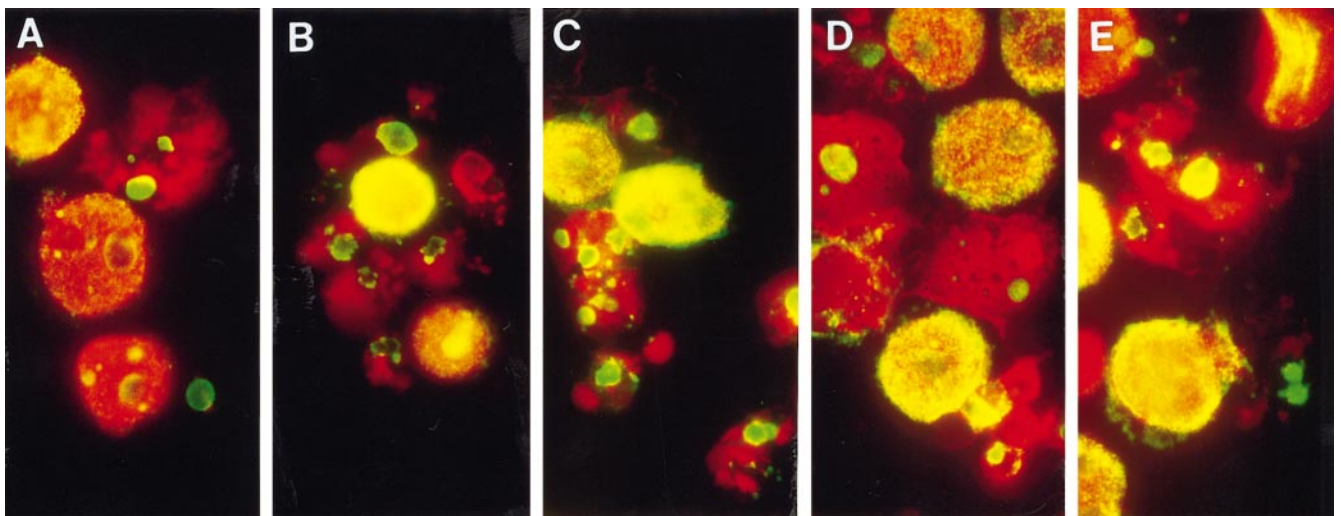


FIG. 4. Separation of RNA from DNA at different stages of apoptosis. Apoptosis of HL-60 cells was induced by treatment either with $\text{TNF-}\alpha$ + CHX for 1.5 h (A-C) or with CPT for 3 h (D, E). Prior to addition of these inducers of apoptosis cellular RNA was pre-labeled by incubation with BrU for 6 h (A, D) or 12 h (B, C, E).

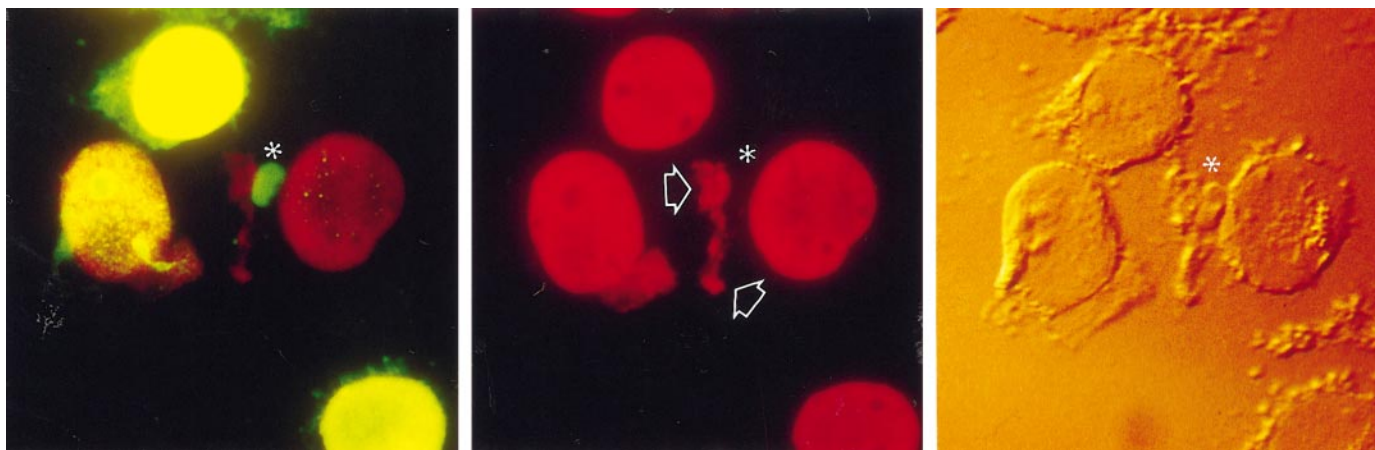


FIG. 5. Separate packaging of RNA and DNA into apoptotic bodies. RNA in HL-60 cells was pre-labeled with BrU for 12 h and the cells were treated with $\text{TNF-}\alpha$ + CHX for 2 h, fixed, and stained with 7-AAD and anti-BrU mAb, which then was detected with FITC-labeled secondary Ab. The cells were examined under fluorescence microscope using blue light illumination, which excites both 7-AAD and FITC (left) and green light illumination that excites only 7-AAD (middle). The right shows the same field under Nomarski interference contrast illumination. Note three apoptotic bodies, one containing only RNA (marked with the asterisk above it) and the other two bodies that contain only DNA (marked with the arrows).

ined under fluorescence microscope using blue light illumination, which excited both 7-AAD and FITC (Fig. 5, left), a distinctly green-fluorescing apoptotic body was apparent (asterisk) while the two adjacent apoptotic bodies showed weak red fluorescence. Upon illumination with green light, i.e., when the excitation of 7-AAD was more efficient compared to blue light, while FITC was not excited, the red fluorescence of the two apoptotic bodies become more intensive (arrows) but no red fluorescence was detectable in the adjacent apoptotic body that was labeled with FITC. The interference contrast illumination confirmed that all three objects were indeed apoptotic bodies, located outside the intact cells (Fig. 5, right).

Quantitative analysis of several hundred individual apoptotic bodies selected based on their total separation from the neighboring cells by interference microscopy (as shown in Fig. 5) revealed that in over 90% of them there was no colocalization of DNA and RNA that could be detected using the combined histochemical (7-AAD) and immunocytochemical (anti-BrU) means of identification of these nucleic acids (Table 1). This was the case in both the CPT and the $\text{TNF-}\alpha$ + CHX-treated cultures following labeling RNA with BrU for different periods of time, between 1 and 24 h.

DISCUSSION

Differential staining of DNA vs RNA in HL-60 or MCF-7 cells undergoing apoptosis revealed that RNA was segregated from DNA, sequestered, and packaged into separate granules which were then packaged into separate apoptotic bodies. The most convincing evidence of the separation of these nucleic acids in the

apoptotic bodies stems from observation of them under the fluorescence microscope following differential staining of RNA with anti-BrU mAb and of DNA with 7-AAD. Over 90% of apoptotic bodies that could be morphologically identified using Nomarski interference contrast had either green (upon excitation with blue light) and no detectable red fluorescence (upon green light excitation) or red and no green fluorescence (Fig. 5; Table 1). Differential staining of RNA vs DNA with Hoechst 33342 and pyronin Y (Fig. 3) confirmed these findings. Most apoptotic bodies, thus, were of the two types: (i) containing RNA and no detectable DNA or (ii) containing DNA and no detectable RNA.

The above findings are consistent with the observations by Biggiogera *et al.* [19, 20], who reported that

TABLE 1

The Percentage of Apoptotic Bodies Containing either RNA or DNA but Not Both Types of Nucleic Acids

Cell treatment	BrU pulse 1 h	BrU pulse 3 h	BrU pulse 24 h
CPT	97 ± 3	96 ± 4	92 ± 6
$\text{TNF-}\alpha$ + CHX	n.d.	96 ± 3	n.d.

Note. HL-60 cells were pre-labeled with BrU for 1, 3, or 24 h and then rinsed free of BrU and incubated in the presence of CPT (for 3 h) or $\text{TNF-}\alpha$ + CHX (2 h). The cells were then cytocentrifuged (1500 rpm, 10 min) and fixed, and the BrU-labeled RNA was detected by anti-BrU mAb and the DNA was counterstained with 7-AAD. Apoptotic bodies were identified under interference contrast and the presence of RNA or DNA in individual bodies was discerned by analyzing their fluorescence upon excitation with either blue or green light, as shown in Fig. 5. The bodies were scored as showing either green (after excitation with blue light) or red (after excitation with green light) but not both colors of fluorescence. n.d., not done.

RNP was excluded from rat thymocytes undergoing spontaneous apoptosis. Their observation was extended in the present study to other cell systems in which apoptosis was induced either along the mitochondrial pathway, by DNA damage with CPT, or along the death receptor pathway, by TNF- α + CHX. By using BrU as a marker of RNA we were able to observe that RNA segregation takes place regardless of the duration of the BrU pulse, from 30 min to 24 h. Because different RNA species have different turnover rates and therefore, depending on length of BrU pulse, are labeled to different degrees, our data suggest that all RNA species that are present in the cell undergo segregation and all end up in the same apoptotic body. Furthermore, the immunocytochemical approach, because it is based on the *combined* evidence of (i) BrU incorporation, (ii) immunoreactivity with the anti-BrU mAb, and (iii) sensitivity to RNase, offers higher specificity in identification of RNA than the histochemical procedure utilizing terbium ions [19]. We have been unable, however, to see the numerous minute structures containing RNA detaching from the single cell by the "blebbing" of the plasma membrane structure as described by Biggiogera *et al.* [19]. Instead, we observed that RNA was present in a single or in two distinct and relatively large apoptotic bodies.

It appears that the RNA separation during apoptosis was initiated by segregation of nucleoli. Nucleolar segregation defines separation and condensation of the granular and dense fibrillar nucleolar components, the structures known to be composed of RNA, from the central fibrillar component that contains DNA (for reviews, [32–34]). Nucleolar segregation was frequently observed following the treatment with different types of anti-tumor drugs, in particular with the intercalators, many of them DNA topoisomerase I or II inhibitors [35–39]. It was assumed that nucleolar segregation induced by anti-tumor drugs is a specific cell response to these drugs in terms of modulation of chromatin and nucleolar structure [33, 35, 37]. However, it was noticed that nucleolar segregation occurs during apoptosis [2–4] in which it appears to be an early morphological change and a characteristic feature ("hallmark") of this mode of cell death [36]. The early changes in cell nucleoli that we observed in the present study are consistent with nucleolar segregation. Nucleolar segregation, thus, by initiating the overall process of separation of RNA from DNA during apoptosis, induced by different anti-tumor drugs including DNA topoisomerase inhibitors, may be a manifestation of apoptosis triggered by these drugs rather than being related to the specific mechanisms by which they modulate chromatin and nucleolar structure [33, 35, 37]. It should be noted that activation of caspase-3 during apoptosis, detected by cleavage of poly(ADP-ribose)

polymerase, is the most prominent in the nucleolus and at the perinucleolar sites [40].

The changes in localization of RNA observed in the present study suggest that simultaneous with—or subsequent to—nucleolar segregation all RNA from nucleoplasm was translocated and aggregated together with the nucleolar RNA. The increased RNA density in the site of its aggregation in the nucleus was reflected by the increased local intensity of the anti-BrU-associated green fluorescence. Progressively, this site became enlarged and underwent demarcation forming a granular structure that was separated from the remaining nuclear fragments. Because at this stage RNA disappeared from the cytoplasm it is likely that the cytoplasmic RNA was translocated and aggregated within the same site. It is possible, however, that cytoplasmic RNA was released separately from the cell in the form of the minute RNP granules as described by Biggiogera *et al.* [19], which were too small to sediment on slides during cytocentrifugation and therefore were not detected.

As mentioned in the Introduction degradation of rRNA during apoptosis by 2',5'-A-dependent RNase L is incomplete, leaving 18S rRNA intact and 28S rRNA cleaved in few sites only [15, 16, 41]. The RNA-binding and RNP-associated proteins, including hnRNP proteins C1 and C2, components of the proteasome, and the 70-kDa component of the U1 small ribonucleoprotein [42–45], are specifically cleaved by caspases. Little is known about the fate of mRNA or tRNA during apoptosis but given the fact that rRNA is cleaved incompletely it is likely that autonomous degradation of the former RNAs may also be incomplete. Completion of RNA degradation, thus, is expected to occur in phagosomes of the cells that phagocytized apoptotic bodies. Packaging RNA into separate granules suggests that the phagosomes of the cells that ingest apoptotic bodies are specialized: some are responsible for DNA degradation, others for degradation of RNA. Such specialization may facilitate heterophagic degradation of nucleic acids. It has been suggested that incomplete degradation of RNP during apoptosis results in development of autoantibodies targeted to RNP-associated autoantigens and may lead to autoimmune disorders [46, 47]. The specialization of phagosomes may also be of relevance in defense mechanisms against RNA and DNA viruses.

This work was supported by NCI Grant CA 28704, the Chemotherapy Foundation, and the "This Close" Foundation for Cancer Research.

REFERENCES

1. Kerr, J. F. R., Wyllie, A. H., and Currie, A. R. (1972). Apoptosis: A basic biological phenomenon with wide-ranging implications in tissue kinetics. *Br. J. Cancer* **26**, 239–257.

2. Wyllie, A. H. (1992). Apoptosis and the regulation of cell numbers in normal and neoplastic tissues: An overview. *Cancer Metastasis Rev.* **11**, 95–103.
3. Kerr, J. F. R., Winterford, C. M., and Harmon, V. (1994). Apoptosis: Its significance in cancer and cancer therapy. *Cancer* **73**, 2013–2026.
4. Majno, G., and Joris, I. (1995). Apoptosis, oncosis, and necrosis. An overview of cell death. *Am. J. Pathol.* **146**, 3–16.
5. Fadok, V. A., Voelker, D. R., Cammpbell, P. A., Cohen, J. J., Bratton, D. L., and Henson, P. M. (1992). Exposure of phosphatidylserine on the surface of apoptotic lymphocytes triggers specific recognition and removal by macrophages. *J. Immunol.* **148**, 2207–2216.
6. Compton, M. M. (1992). A biochemical hallmark of apoptosis: Internucleosomal degradation of the genome. *Cancer Metastasis Rev.* **11**, 105–119.
7. Ueda, N., Walker, P. D., Hsu, S.-M., and Shah, S. V. (1995). Activation of a 15-kDa endonuclease in hypoxia/reoxygenation injury without morphologic features of apoptosis. *Proc. Natl. Acad. Sci. USA* **92**, 7202–7206.
8. Liu, Q. Y., Ribocco, M., Pandey, S., Walker, P. R., and Sikorska, M. (1999). Apoptosis-related functional features of the DNase I-like family of nucleases. *Ann. N. Y. Acad. Sci.* **887**, 60–76.
9. Nagata, S. (2000). Apoptotic DNA fragmentation. *Exp. Cell Res.* **256**, 12–18.
10. Enari, M., Sakahira, H., Yokoyama, H., Okawa, K., Iwamatsu, A., and Nagata, S. (1998). A caspase-activated DNase that degrades DNA during apoptosis and its inhibitor ICAD. *Nature* **391**, 43–50.
11. Liu, X., Zou, H., Slaughter, C., and Wang, X. (1997). DFF, a heterodimeric protein that functions downstream of caspase-3 to trigger DNA fragmentation during apoptosis. *Cell* **89**, 175–184.
12. Ferri, K. F., and Kroemer, G. (2000). Control of DNA degradation. *Nat. Cell Biol.* **2**, E63–E64.
13. Wu, Y.-C., Stanfield, G. M., and Horvitz, H. R. (2000). NUC-1, a *Caenorhabditis elegans* DNase II homolog, functions in an intermediate step of DNA degradation during apoptosis. *Genes Dev.* **14**, 536–548.
14. McIlroy, D., Tanaka, M., Sakahira, H., Fukuyama, H., Suzuki, M., Yamamura, K., Ohsawa, Y., Uchiyama, Y., and Nagata, S. (2000). An auxiliary mode of apoptotic DNA fragmentation provided by phagocytes. *Genes Dev.* **14**, 549–558.
15. Diaz-Guerra, M., Rivas, C., and Esteban, M. (1997). Activation of the INF-inducible enzyme RNase L causes apoptosis of animal cells. *Virology* **236**, 354–363.
16. Castelli, J. C., Hassel, B., Maran, A., Paranjape, J., Hewitt, J. A., Li, X.-I., Hsu, Y.-T., Silverman, R. H., and Youle, R. J. (1998). The role of 2'-5' oligoadenylate-activated ribonuclease L in apoptosis. *Cell Death Differ.* **5**, 313–320.
17. Houge, G., Robaye, B., Eikhom, T. S., Golstein, J., Mellgren, G., Gjertsen, B. T., Lanotte, M., and Doskeland, S. O. (1995). Fine mapping of 28S rRNA sites specifically cleaved in cells undergoing apoptosis. *Mol. Cell. Biol.* **15**, 2051–2062.
18. Nadano, D., and Sato, T.-A. (2000). Caspase-3-dependent and -independent degradation of 28 S ribosomal RNA may be involved in the inhibition of protein synthesis during apoptosis initiated by death receptor engagement. *J. Biol. Chem.* **275**, 13967–13973.
19. Biggiogera, M., Bottone, M. G., and Pellicciari, C. (1998). Nuclear RNA is extruded from apoptotic cells. *J. Histochem. Cytochem.* **46**, 999–1005.
20. Biggiogera, M., Bottone, M. G., Martin, T. E., Uchimi, T., and Pellicciari, C. (1997). Still immunodetectable nuclear RNPs are extruded from the cytoplasm of spontaneously apoptotic thymocytes. *Exp. Cell Res.* **234**, 512–520.
21. Jensen, P. Ø., Larsen, J., and Larsen, J. K. (1993). Flow cytometric measurement of RNA synthesis using bromouridine labeling and bromodeoxyuridine antibodies. *Cytometry* **14**, 455–458.
22. Haider, S. R., Juan, G., Traganos, F., and Darzynkiewicz, Z. (1997). Immunoseparation and immunodetection of nucleic acids labeled with halogenated nucleotides. *Exp. Cell Res.* **234**, 488–506.
23. Larsen, J. K., Jensen, P. Ø., and Larsen, J. (2000). Flow cytometric analysis of RNA synthesis by detection of bromouridine incorporation. In "Current Protocols in Cytometry" (J. P. Robinson, Z. Darzynkiewicz, P. Dean, A. Orfao, P. Rabinovitch, and H. Tanke, Eds.), pp. 7.12.1–7.12.11, Wiley, New York.
24. Shapiro, H. M. (1981). Flow cytometric estimation of DNA and RNA content in intact cells stained with Hoechst 33342 and pyronin Y. *Cytometry* **2**, 143–150.
25. Darzynkiewicz, Z., Kapuscinski, J., Traganos, F., and Crissman, H. A. (1987). Application of pyronin Y in cytochemistry of nucleic acids. *Cytometry* **8**, 138–145.
26. Kametsky, L. A., Burger, D. E., Gershman, R. J., Kametsky, L. D., and Luther, E. (1997). Slide-based laser scanning cytometry. *Acta Cytol.* **41**, 123–143.
27. Darzynkiewicz, Z., Bedner, E., Li, X., Gorczyca, W., and Melamed, M. R. (1999). Laser scanning cytometry. A new instrumentation with many applications. *Exp. Cell Res.* **249**, 1–12.
28. Bedner, E., Smolewski, P., Amstad, P., and Darzynkiewicz, Z. (2000). Activation of caspases measured *in situ* by binding of fluorochrome-labeled inhibitors of caspases (FLICA): Correlation with DNA fragmentation. *Exp. Cell Res.* **259**, 308–313.
29. Bedner, E., Li, X., Gorczyca, W., Melamed, M. R., and Darzynkiewicz, Z. (1999). Analysis of apoptosis by laser scanning cytometry. *Cytometry* **35**, 181–195.
30. Li, X., Patel, R., Melamed, M. R., and Darzynkiewicz, Z. (1994). The cell cycle effects and induction of apoptosis by 5-bromouridine in cultures of human leukemic MOLT-4 and HL-60 cell lines and mitogen stimulated normal lymphocytes. *Cell Prolif.* **27**, 307–320.
31. Bruno, S., Bauer, K., Crissman, H. A., and Darzynkiewicz, Z. (1991). Changes in cell nuclei during S phase: Progressive chromatin condensation and altered expression of the proliferation-associated nuclear proteins Ki-67, p-105, cyclin/PCNA, and p34. *Exp. Cell Res.* **196**, 99–106.
32. Ghosh, S. (1987). The nucleolus. *Int. Rev. Cytol.* **17**(Suppl.), 573–588.
33. Brasch, K. (1990). Drug and metabolite-induced perturbations in nuclear and nucleolar function. A review. *Biochem. Cell. Biol.* **68**, 408–426.
34. Pederson, T. (1999). Movement and localization of RNA in the cell nucleus. *FASEB J.* **2**(Suppl.), S238–S2442.
35. Imazawa, T., Nishikawa, A., Tada, M., Takahashi, M., and Hayashi, Y. (1995). Nucleolar segregation as an early marker for DNA damage: An experimental study in rats treated with 4-hydroxyaminoquinolone 1-oxide. *Virchows Arch.* **426**, 295–300.
36. Raipert, S., Bennion, G., Hickman, J. A., and Allen, T. D. (1999). Nucleolar segregation during apoptosis of hematopoietic stem cell line FDCP-Mix. *Cell Death Differ.* **6**, 334–341.
37. Kapuscinski, J., and Darzynkiewicz, Z. (1986). Relationship between the pharmacological activity of antitumor drugs Amet-

- antrone and Mitoxantrone (Novatrone) and their ability to condense nucleic acids. *Proc. Natl. Acad. Sci. USA* **83**, 6302–6306.
38. Krajci, D., Mares, V., Lisa, V., Spanova, A., and Vorlicek, J. (2000). Ultrastructure of nuclei of cisplatin-treated C6 glioma cells undergoing apoptosis. *Eur. J. Cell Biol.* **79**, 365–376.
 39. Jensen, C. G., Wilson, W. R., and Bleumink, A. R. (1985). Effects of amsacrine and other DNA-intercalating drugs on nuclear and nucleolar structure in cultured V79 Chinese hamster cells and PtK2 rat kangaroo cells. *Cancer Res.* **45**, 717–725.
 40. Li, X., and Darzynkiewicz, Z. (2000). Cleavage of poly(ADP-ribose) polymerase measured *in situ* in individual cells: Relationship to DNA fragmentation and cell cycle position during apoptosis. *Exp. Cell Res.* **255**, 125–132.
 41. Diaz-Guerra, M., Rivas, C., and Esteban, M. (1999). Full activation of RNaseL in animal cells requires binding of 2-5A within ankyrin repeats 6 to 9 of this interferon-inducible enzyme. *J. Interferon Cytokine Res.* **19**, 113–119.
 42. Degan, W. G., Aarsen, Y., Pruijn, G. J., and van Venrooij, W. J. (2000). The fate of U1 snRNP during anti-Fas induced apoptosis: Specific cleavage of the U1 snRNA molecule. *Cell Death Differ.* **7**, 70–79.
 43. Waterhouse, N., Kumar, S., Song, Q., Strike, P., Sparrow, L., Dreyfuss, G., Alnemri, E., Litwack, G., Lavin, M., and Waters, D. (1996). Heteronuclear ribonucleoproteins C1 and C2, components of the spliceosome, are specific targets of interleukin 1beta-converting enzyme-like proteases in apoptosis. *J. Biol. Chem.* **271**, 29335–29341.
 44. Rickers, B. E., Kostka, A., Laubersheimer, A., Dorken, B., Wittman-Liebhold, B., Bommert, K., and Otto, A. (1998). Identification of apoptosis-associated proteins in a human Burkitt lymphoma cell line. Cleavage of heterogeneous nuclear ribonucleoprotein A1 by caspase 3. *J. Biol. Chem.* **273**, 28057–28064.
 45. Martelli, A. M., Robuffo, I., Bortul, R., Ochs, R. L., Lauchetti, R., Cocco, L., Zweyer, M., Beroggi, R., and Falcieri, E. (2000). Behavior of nuclear proteins during the course of apoptosis in camptothecin-treated HL-60 cells. *J. Cell. Biochem.* **78**, 264–277.
 46. Casciola-Rosen, L. A., Anhalt, G., and Rosen, A. (1994). Autoantigens targeted in systemic lupus erythematosus are clustered in two populations of surface structures on apoptotic keratinocytes. *J. Exp. Med.* **179**, 1317–1330.
 47. Van Venroij, W. J., and Pruijn, G. J. (1995). Ribonucleoprotein complexes as autoantigens. *Curr. Opin. Immunol.* **7**, 819–824.

Received July 21, 2000

Revised version received August 16, 2000